The Journal of Experimental Biology 210, 3848-3861
Published by The Company of Biologists 2007
doi:10.1242/jeb.007872

Molecular cloning, phylogeny and localization of AgNHA1: the first Na^+/H^+ antiporter (NHA) from a metazoan, *Anopheles gambiae*

Mark R. Rheault[1,*], Bernard A. Okech[1], Stephen B. W. Keen[2], Melissa M. Miller[1], Ella A. Meleshkevitch[3], Paul J. Linser[1], Dmitri Y. Boudko[3] and William R. Harvey[1,†]

[1]*The Whitney Laboratory for Marine Bioscience, University of Florida, 9505 Ocean Shore Boulevard, St Augustine, FL 32080, USA,* [2]*Wake Forest University School of Medicine, Winston-Salem, NC 27157, USA and* [3]*Rosalind Franklin University of Medicine and Science, North Chicago, IL 60064, USA*

*Present address: University of British Columbia Okanagan, Kelowna, BC, V1V 1V7, Canada
†Author for correspondence (e-mail: wharvey@whitney.ufl.edu)

Accepted 20 August 2007

Summary

We have cloned a cDNA encoding a new ion transporter from the alimentary canal of larval African malaria mosquito, *Anopheles gambiae* Giles *sensu stricto*. Phylogenetic analysis revealed that the corresponding gene is in a group that has been designated NHA, and which includes (Na^+ or K^+)/H^+ antiporters; so the novel transporter is called AgNHA1. The annotation of current insect genomes shows that both AgNHA1 and a close relative, AgNHA2, belong to the cation proton antiporter 2 (CPA2) subfamily and cluster in an exclusive clade of genes with high identity from *Aedes aegypti*, *Drosophila melanogaster*, *D. pseudoobscura*, *Apis mellifera* and *Tribolium castaneum*. Although NHA genes have been identified in all phyla for which genomes are available, no NHA other than AgNHA1 has previously been cloned, nor have the encoded proteins been localized or characterized.

The AgNHA1 transcript was localized in *An. gambiae* larvae by quantitative real-time PCR (qPCR) and *in situ* hybridization. AgNHA1 message was detected in gastric caeca and rectum, with much weaker transcription in other parts of the alimentary canal. Immunolabeling of whole mounts and longitudinal sections of isolated alimentary canal showed that AgNHA1 is expressed in the cardia, gastric caeca, anterior midgut, posterior midgut, proximal Malpighian tubules and rectum, as well as in the subesophageal and abdominal ganglia.

A phylogenetic analysis of NHAs and KHAs indicates that they are ubiquitous. A comparative molecular analysis of these antiporters suggests that they catalyze electrophoretic alkali metal ion/hydrogen ion exchanges that are driven by the voltage from electrogenic H^+ V-ATPases. The tissue localization of AgNHA1 suggests that it plays a key role in maintaining the characteristic longitudinal pH gradient in the lumen of the alimentary canal of *An. gambiae* larvae.

Key words: sodium, potassium, exchanger, alkalinization, AgNHA, NHA, AgNHE, NHE, CHA, CHE, CPA2, African malaria mosquito.

Introduction

All organisms regulate their cellular pH, volume and ionic composition. Na^+ and H^+ play key roles in all of these physiological processes; hence regulation of their intracellular concentrations is vital for protein and cell functions. All cells from bacteria to higher vertebrates have at least one transporter that is capable of exchanging intracellular H^+ for extracellular Na^+. In vertebrates this exchange is thought to be mediated by Na^+/H^+ exchanger (NHE) proteins, whose stoichiometry is $1Na^+/1H^+$; the exchange is therefore electroneutral and is independent of transmembrane voltages. The energy that drives this secondary exchange is provided by the inwardly directed Na^+ gradient that is generated from the hydrolysis of ATP by primary Na^+/K^+ P-ATPases (Skou, 1990).

In contrast to this electroneutral secondary $1Na^+/1H^+$ exchange of eukaryotic cells, secondary Na^+/nH^+ exchange in prokaryotic cells, such as the bacterium *Escherichia coli*, is electrophoretic[1]. Na^+/nH^+ antiporters (NhaA, NhaB) use the voltage gradient that is generated by an H^+ F-ATPase to drive the uptake of hydrogen ions and expulsion of sodium ions (Padan et al., 2001). This transport is in the opposite direction

[1]A process that is driven by a voltage is said to be 'electrophoretic' whereas a process that generates a voltage is said to be 'electrogenic'. H^+ F-ATPases and H^+ V-ATPases are electrogenic because they drive hydrogen cations (H^+) across biomembranes with no accompanying anion (A^-). The result is that (+) charges accumulate on the outside and (–) charges on the inside of plasma membranes, rendering the inside electrically negative to the outside: the plasma membrane is said to be hyperpolarized or 'energized' (Harvey, 1992). Just as an outside-high Na^+ concentration difference, $\Delta[Na^+]$, can drive Na^+ into cells, an outside-positive potential difference, $\Delta\Psi$, can also drive Na^+ into cells. For example, an 18 mV $\Delta\Psi$ is roughly equivalent to a twofold $\Delta[Na^+]$; a 60 mV $\Delta\Psi$ to a tenfold $\Delta[Na^+]$ etc. Alan Hodgkin has said that a concentration is like fleas hopping and a voltage is like fleas hopping in a breeze. In many animal cells the phosphorylation potential predicts that a voltage generated by a plasma membrane ATPase can exceed 240 mV, equivalent to a 10 000-fold $\Delta[Na^+]$ (Harvey et al., 1983b).

from that of vertebrate NHEs and enables *E. coli* to survive in hyper saline and/or alkaline environments (Padan et al., 2005).

Evidence that electroneutral Na^+/H^+ exchangers (NHE) are present in epithelia and neural tissues of invertebrates is available from molecular cloning studies (Gaillard and Rodeau, 1987; Kang'ethe et al., 2007; Pullikuth et al., 2006; Schlue and Thomas, 1985; Strauss and Graszynski, 1992). By contrast, evidence for electrophoretic Na^+/H^+ antiporters (NHA) is derived only from functional studies on isolated membrane vesicles. In crustaceans, acidification of the alimentary canal and Na^+ absorption by the gills is mediated by an antiporter that exchanges two extracellular Na^+ ions for one intracellular H^+ (Ahearn and Clay, 1989; Ahearn and Franco, 1991). A similar antiporter has been identified in vesicle studies on an echinoderm (Shetlar and Towle, 1989).

A second type of electrophoretic antiporter was first identified in goblet cell apical membrane vesicles from the midgut of the larval tobacco hornworm *Manduca sexta* (Wieczorek et al., 1991). Neither a Na^+/K^+-ATPase nor Na^+ gradients that could drive a secondary cation exchanger have been detected in the caterpillar midgut (Dow et al., 1984; Harvey et al., 1983a). Instead, a large voltage gradient (Dow and Peacock, 1989), generated by an H^+ V-ATPase (Wieczorek et al., 1989), is thought to drive the exchange of two extracellular H^+ for one intracellular K^+ (Azuma et al., 1995), an exchange that is believed to maintain the highly alkaline pH in anterior midgut (Harvey et al., 1983a; Lepier et al., 1994; Wieczorek, 1992). The lepidopteran midgut was the first animal organ in which the voltage generated by a primary proton pump was shown to provide the driving force for secondary transport across a plasma membrane (Klein, 1992).

The anterior midgut lumen of mosquitoes is also very alkaline (Dadd, 1975) and ion-transporting membranes in many of its cells are studded with portasomes (Volkmann and Peters, 1989b; Zhuang et al., 1999), which are now known to be V_1-ATPase particles (Grüber et al., 2000). Does the voltage generated by these H^+ V-ATPases provide energy for the alkalinization? It is tempting to suggest that the Na^+/H^+ exchangers in the alkaline midgut of insects function like those previously characterized in prokaryotes and are an adaptation for function in an alkaline environment. The caterpillar antiporter translocates H^+ inwardly and (K^+ or Na^+) outwardly using a voltage gradient rather than a sodium ion gradient to drive the exchange. The similarity between insects and alkalophilic bacteria was noted by Lepier et al. (Lepier et al., 1994), who speculated that the resemblance may result from a common ancestor rather than from convergent evolution. Although transcripts of genes encoding the Na^+/K^+ P-ATPase, the H^+ V-ATPase and the electroneutral NHEs have been cloned from many animal tissues, no electrophoretic (Na^+ or K^+)/nH^+ antiporter has previously been cloned from an animal tissue.

The rapid increase in genomic information has made it possible to identify genes encoding potential insect electrophoretic Na^+/H^+ antiporters *in silico* (Giannakou and Dow, 2001). Using available genomes, all predicted alkali metal ion/hydrogen ion exchangers and antiporters have been redefined and placed in a single superfamily based on phylogeny (Chang et al., 2004; Brett et al., 2005). This new clade is called the monovalent Cation Proton Antiport (CPA) superfamily. The Transport Protein Database (http://www.tcdb.org) subdivides the CPA superfamily into three subfamilies; CPA1 (TC#2.A.36), CPA2 (TC#2.A.37) and the Na^+-transporting carboxylic acid decarboxylase family (NaT-DC: TC#3.B.1). This third subfamily comprises only prokaryotic representatives and will not concern us further. The CPA1 gene family includes all of the electroneutral NHEs that have been well characterized in plants, fungi and animals by molecular techniques. The CPA2 family is composed of a number of prokaryotic members including the well characterized *E. coli* NhaA and NhaB, and also includes genes predicted but not cloned or characterized in all animal genomes including those of *Homo sapiens* and *Anopheles gambiae*. Thus, the CPA2 gene subfamily provides great promise for the identification, molecular cloning, localization and characterization of electrophoretic transporters, not just in insects, but throughout all of the eukaryotic phyla.

The present manuscript reports the molecular cloning and phylogeny of the first animal member of the CPA2 gene family, describes its characteristics, reports the localization pattern of its RNA transcripts and encoded proteins and designates it as AgNHA1. We propose that AgNHA1 is electrophoretic and support this hypothesis indirectly by structural and phylogenetic evidence. It is supported directly by unpublished electrical data (L. B. Popova, D.Y.B. and W.R.H.) from AgNHA1-transfected *Xenopus laevis* oocytes; these data include increase in inward currents with lowered pH, as measured with 2-electrode voltage clamps and slowed acidification by ammonium chloride, as measured with ion-selective intracellular microelectrodes.

Materials and methods

Rearing of larvae

An. gambiae Giles *sensu stricto* (Diptera, Culicidae, G3 strain) eggs were supplied by MR4 (The Malaria Research and Reference Reagents Resource Center) at the Centers for Disease Control and Prevention in Atlanta, GA, USA (http//www.malaria.atcc.org), and raised to the fourth instar as described in the supplier manual (www2.ncid.cdc.gov/vector/vector.html) under a 12 h:12 h dark:light interval and 2 day feeding schedule.

Cloning of full-length cDNA encoding AgNHA1

A predicted NHE-like coding sequence fragment (GenBank accession number XM_320946) was identified in a targeted BLAST search of the *An. gambiae* genome. Both 5′ and 3′ RACE were performed on an amplified cDNA collection constructed from a pool of midgut tissue that was isolated from *An. gambiae* fourth instar larvae (Matz, 2002). A full-length sequence was obtained and designated *Anopheles gambiae* Na^+/H^+ antiporter 1 (AgNHA1; GenBank accession number EF014219) using terminal primers: 5′-ATTATCAAGA-TGCCTTCGGAGGAA-3′ and 5′-CTACTTCGTGATGGTG-AACGCTGTCGCCGTTT-3′. The resulting PCR product was inserted into a pCR4-TOPO vector (Invitrogen, Carlsbad, CA, USA) and sequenced to verify that no PCR errors had been introduced, using methods that were described earlier (Meleshkevitch et al., 2006).

Table 1. *Proteins used for sequence alignment and phylogenetic analysis of the CPA transporter family*

Protein	Species	Accession no.	Protein	Species	Accession no.
EcNHaA	*Escherichia coli*	NP_414560	DmNHE1	*Drosophila melanogaster*	NP_608491
CtNHA1	*Clostridium thermocellum*	ZP_00503701	AgNHE1	*Anopheles gambiae*	XP_307859
CteNHA1	*Clostridium tetani*	NP_782716	AeNHE1	*Aedes aegypti*	EAT44116
AbNHA	*Alkaliphilus metalliredigenes*	ZP_00799803	HsNHE2	*Homo sapiens*	Q9UBY0
MtNHA1	*Methanothermobacter thermautotrophicus*	NP_275902	RnNHE2	*Rattus norvegicus*	P48763
MmNHA1	*Mus musculus*	BAC26494	MmNHE2	*Mus musculus*	NP_001028461
RnNHA1	*Rattus norvegicus*	XP_001077752	DmNHE2	*Drosophila melanogaster*	NP_724311
CfNHA1	*Canis familiaris*	XP_535675	AgNHE2	*Anopheles gambiae*	AAO34131
HsNHA1	*Homo sapiens*	XP_208142	AeNHE2	*Aedes aegypti*	AAM63432
RhNHA1	*Macaca mulatta*	XP_001110224	HsNHE3	*Homo sapiens*	AAI01670
CeNHA1	*Caenorhabditis elegans*	NP_509724	RnNHE3	*Rattus norvegicus*	NP_036786
CbNHA1	*Caenorhabditis briggsae*	CAE70554	MmNHE3	*Mus musculus*	XP_998126
TcNHA1	*Tribolium castaneum*	XP_974978	AgNHE3	*Anopheles gambiae*	XP_314826
AmNHA1	*Apis mellifera*	XP_394256	DmNHE3	*Drosophila melanogaster*	NP_609064
DsNHA1	*Drosophila pseudoobscura*	EAL32825	HsNHE4	*Homo sapiens*	NP_001011552
DmNHA1	*Drosophila melanogaster*	NP_723224	RnNHE4	*Rattus norvegicus*	NP_775121
AgNHA1	*Anopheles gambiae*	ABJ91581	MmNHE4	*Mus musculus*	AAI20544
AeNHA1	*Aedes aegypti*	EAT48854	HsNHE5	*Homo sapiens*	Q14940
CfNHA2	*Canis familiaris*	XP_852596	RnNHE5	*Rattus norvegicus*	NP_620213
MmNHA2	*Mus musculus*	NP_849208	MmNHE5	*Mus musculus*	XP_920472
RnNHA2	*Rattus norvegicus*	XP_001075654	HsNHE6	*Homo sapiens*	NP_001036002
HsNHA2	*Homo sapiens*	NP_849155	RnNHE6	*Rattus norvegicus*	XP_001053956
RhNHA2	*Macaca mulatta*	XP_001110438	MmNHE6	*Mus musculus*	NP_766368
CeNHA2	*Caenorhabditis elegans*	NP_509723	HsNHE7	*Homo sapiens*	NP_115980
CbNHA2	*Caenorhabditis briggsae*	CAE70553	RnNHE7	*Rattus norvegicus*	XP_001055038
AmNHA2	*Apis mellifera*	XP_001121694	MmNHE7	*Mus musculus*	Q8BLV3
DmNHA2	*Drosophila melanogaster*	NP_732807	HsNHE8	*Homo sapiens*	Q9Y2E8
AgNHA2	*Anopheles gambiae*	XP_312647	RnNHE8	*Rattus norvegicus*	NP_001020452
AeNHA2	*Aedes aegypti*	EAT36864	MmNHE8	*Mus musculus*	NP_683731
HsNHE1	*Homo sapiens*	NP_003038	HsNHE9	*Homo sapiens*	BAD69592
RnNHE1	*Rattus norvegicus*	NP_036784	RnNHE9	*Rattus norvegicus*	XP_001064905
MmNHE1	*Mus musculus*	AAH51431	MmNHE9	*Mus musculus*	NP_808577

Accession numbers are from GenBank.

AgNHA1 structure

Amino acid sequences were aligned using ClustalX (v1.81) (Thompson et al., 1997) with final shading and graphical output by Genedoc (Nicholas et al., 1997). The relative molecular mass of AgNHA1 was calculated using the Compute pI/Mw tool (Gasteiger et al., 2005). The secondary structures of AgNHA1, AeNHA1, DsNHA1, DmNHA1, TcNHA1 and AmNHA1 were predicted using hydrophobicity analysis [TopPred tool: (Claros and von Heijne, 1994; von Heijne, 1992)] and the Goldman–Engelman–Steitz hydrophobicity scale. Potential protein family (Pfam) domains were predicted using the Simple Modular Architecture Research Tool [SMART (Schultz et al., 1998)]. Potential phosphorylation sites were predicted using phosphorylation consensus motifs (Pearson and Kemp, 1991) and the PROSITE scan tool (Sigrist et al., 2002). Potential glycosylation sites were predicted using the criteria of Gavel and Heijne (Gavel and Heijne, 1990) and PROSITE.

Phylogeny of NHAs

Representative amino acid sequences from NHE (CPA1) and NHA (CPA2) subfamilies were retrieved from the GenBank database (Table 1). *Escherichia coli* NhaA was used as an outgroup for construction of a phylogenetic tree which was generated using default parameters and 100 000 iterations of the maximum likelihood algorithm implemented in the program TREE-PUZZLE (v5.0) (Schmidt et al., 2002). The initial multiple alignment used ClustalX (ver1.81) (Thompson et al., 1997) with default parameters; all gaps were removed manually using GeneDoc (Nicholas et al., 1997) prior to tree construction. The graphical output was generated using TreeView software (Page, 1996) (for details, see Meleshkevitch et al., 2006).

Whole-mount in situ hybridization

A purified AgNHA1/pCR4-TOPO plasmid was linearized using *Not*I or *Spe*I restriction enzymes (New England Biolabs; Ipswich, MA, USA) to obtain full-length, run-off transcripts, using T3 and T7 promoters for antisense and sense probes, respectively. Digoxygenin (DIG)-labeled probes were transcribed *in vitro* using a DIG RNA labeling kit (Roche Diagnostics, Mannheim, Germany). Tissues were pre-fixed, isolated from fourth instar *An. gambiae* larvae, pre-hybridized, hybridized, fixed and labeled with alkaline phosphatase-conjugated, anti-DIG antibodies by a slightly modified version of the methods published (Meleshkevitch et al., 2006). Hybridization patterns were visualized in a NBT/BCIP alkaline buffer solution (Roche Diagnostics). Labeled preparations were fixed in 4% PFA in methanol, embedded in 3:1 glycerol: PBS on glass slides and photographed using an inverted DIAPHOT

300 confocal microscope (Nikon Inc., Melville, NY, USA) equipped with Hoffman contrast optics and a Fuji 2S Pro digital SLR camera. Images were processed and figures prepared using CorelDRAW Graphics Suite X3 (Corel; Ottawa, ON, Canada).

Quantitative real time polymerase chain reaction (qPCR)

RNA isolation, cDNA synthesis, qPCR experiments and data analysis were performed as described (Meleshkevitch et al., 2006). AgNHA1-specific primers designed using Primer Express v.2.0 software (Applied Biosystems; Foster City, CA, USA) had the following sequences: AgNHA1-1105F= CTGGATCCTCACATCGTATCGA; AgNHA1-1176R=CGT-TGTCAAGATGCGGATCA. Transcript abundance of AgNHA1 in each tissue was normalized to values for 18S ribosomal RNA and expressed relative to that found in the carcass, which was set to a value of 1. Data represent three averaged replicates of three independent experiments.

AgNHA1 antibody preparation

A 17-residue sequence of AgNHA1 located in the N-terminal region and another in the extracellular loop between transmembrane domains (TMDs) 11 and 12 were chosen for antibody production. The N-terminal sequence consisting of FSEALEKIERDYDNSRL and the extracellular one consisting of LKTVMSNENRTEEEVHY were synthesized and conjugated to keyhole limpet hemocyanin (KLH; 21st Century Biochemicals, Marlboro, MA, USA). Both synthetic peptide–KLH constructs were emulsified in Freund's complete adjuvant and were injected into a rabbit to elicit immune responses. A serum sample was collected from the rabbit prior to injection to serve as a pre-immune control. Ten weeks after the initial injection serum was collected and tested for IgG antibodies using ELISA. This serum sample was used in western blots and in all immunolocalization experiments.

Western blot analysis of AgNHA1 antibody

Membranes were isolated from whole *An. gambiae* larvae using standard differential centrifugation techniques (Umesh et al., 2003). The isolated membranes were treated with sample loading buffer NuPAGE® LDS (Invitrogen, Carlsbad, CA, USA), 25 μg were loaded per lane on a 4%–12% Bis-Tris polyacrylamide gradient gel (Invitrogen) and the proteins were separated by electrophoresis under reducing conditions. The separated proteins were transferred to a nitrocellulose membrane (0.45 μm; Millipore, Billerica, MA, USA) and the blots were stained with Fast Green to confirm equal loading and transfer and to visualize lane boundaries. Then the blots were cut into strips for probing with various serum samples. Before being probed, the blots were blocked in buffer containing 2.5% non-fat dry milk powder (Carnation®) in Tris buffered saline (TBS) with 0.2% Tween-20 (TBST) for 1 h at room temperature. Then they were incubated with anti-AgNHA1 antibody at a dilution of 1:1000 in blocking buffer overnight at 4°C. The specificity of the AgNHA1 polyclonal antibodies was tested by incubation of control lanes with either pre-immune serum or AgNHA1 antibodies blocked by a 2 h pre-incubation with purified epitopic peptide. Blots were incubated with alkaline phosphatase-coupled goat anti-rabbit IgG (Jackson ImmunoResearch, West Grove, PA, USA) at a dilution of 1:2000 in blocking buffer for 1–2 h at room temperature. Western blots were visualized by the alkaline phosphate color precipitation method and the images were converted to 8-bit gray-scale using ImageJ (Abramoff et al., 2004). The gray-scale image was threshold corrected to normalize all lanes (threshold value=150). The intensity of staining was quantified by measuring pixel area of the bands of interest in the threshold-corrected images.

Immunolocalization of AgNHA1

The entire alimentary canal (AC) was isolated from fourth instar *An. gambiae* larvae as described (Meleshkevitch et al., 2006). Tissues were fixed in 4% paraformaldehyde/PBS (PFA), rinsed in PBS, incubated in an ethanol dehydration/rehydration series, rinsed with PBS containing 0.3% Triton X-100 (PBT) and blocked overnight at 4°C with a solution of 2% normal goat serum (NGS), 1% bovine serum albumin (BSA) in PBT. On the following night issues were incubated at 4°C in a 1:250 dilution of the AgNHA1 polyclonal antibody serum or pre-immune serum (control) in blocking solution. To remove unbound antibody, tissues were rinsed several times with blocking solution. Bound antibody was detected by incubation for 6–12 h at 4°C with a fluorescein isothiocyanate (FITC)-labeled goat anti-rabbit secondary antibody (Invitrogen, Carlsbad, CA, USA) at a 1:500 dilution in blocking solution, followed by a wash step.

Paraffin sections (6 μm thick) were prepared from larval tissues by the method of Patrick et al. (Patrick et al., 2006), mounted onto gelatin-coated slides (1% gelatin and 0.1% chromium potassium sulfate) and allowed to dry. Sections were de-waxed in 100% xylene, rehydrated *via* an ethanol series, washed in distilled water and finally washed in PBT. After incubation in blocking solution for 1 h at room temperature they were exposed to AgNHA1 polyclonal antibodies at 1:250 dilution in blocking solution at 4°C overnight. The following day, sections were washed with blocking solution and then incubated with FITC-labeled goat anti-rabbit secondary antibody (Invitrogen) at a 1:500 dilution for 3 h at room temperature, followed by further washing.

For both whole mounts and paraffin sections, nuclear DNA was visualized by staining with DRAQ 5 (Biostatus Limited, Shepshed, UK) at a dilution of 1:1000 for 5 min before mounting. Tissues were mounted on slides in a solution of 60% glycerol in PBS and examined on a Leica laser scanning confocal microscope (LSCM SP2) or were stored at –20°C in the dark. Captured images were processed with CorelDRAW Graphics Suite X3 (Corel; Ottawa, ON, Canada).

All abbreviations are defined in the List of abbreviations.

Results

AgNHA1 structure

AgNHA1 (GenBank accession number EF014219) has an open reading frame (ORF) of 1944-base pairs (bp) that is 98% identical to the predicted transcript (accession number XM_320946). The sequence deduced from that of the cDNA (top lines, Fig. 1A) corresponds to a 647-amino acid polypeptide with a calculated molecular mass of 70.8 kDa [Compute pI/Mw tool (Gasteiger et al., 2005)]. Hydrophobicity analysis predicts a 151-residue cytosolic N terminus followed by 12 potential transmembrane domains

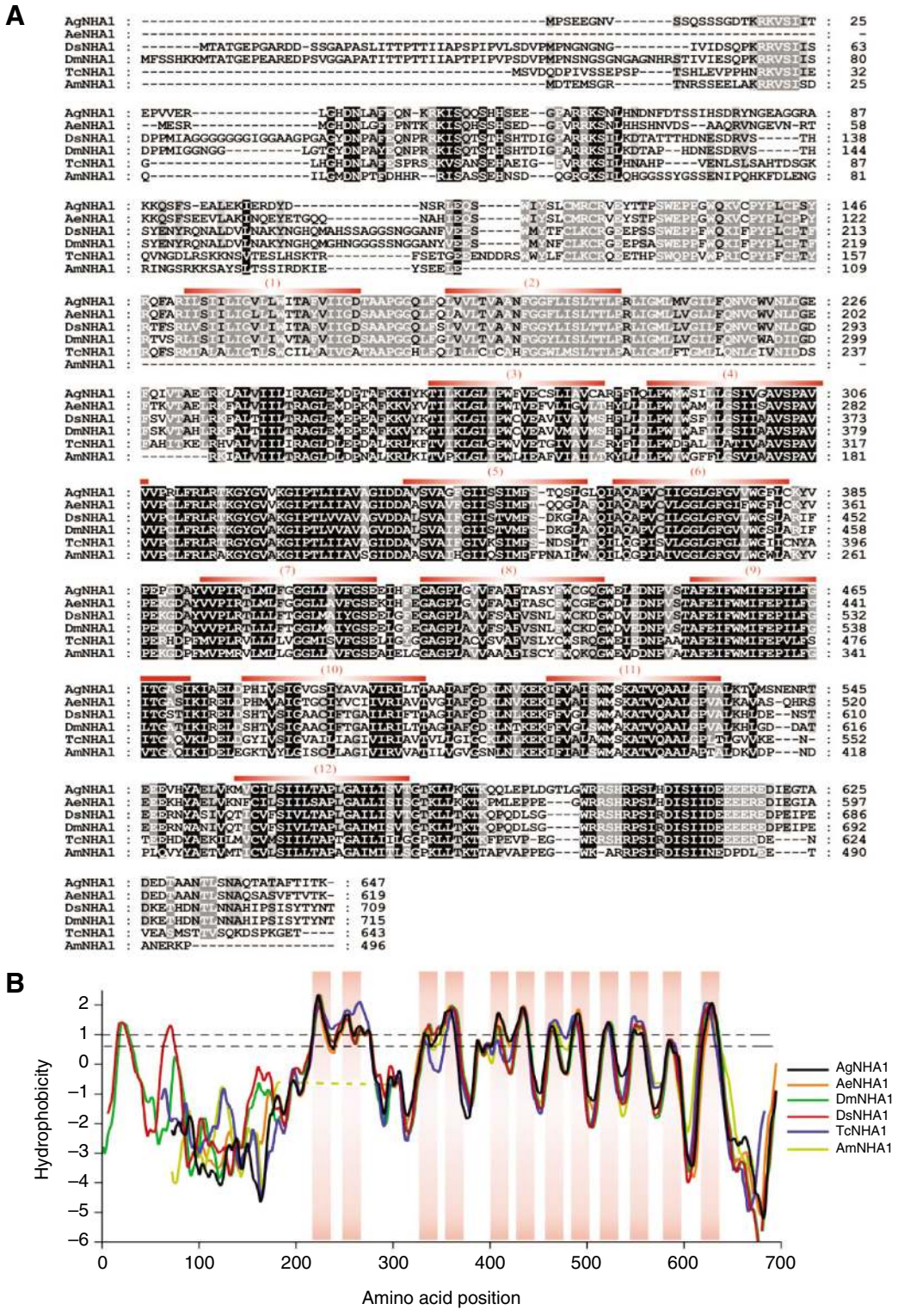

Fig. 1. Comparison of insect NHA1 amino acid sequences. (A) Alignment of AgNHA1 with other predicted insect NHA1 amino acid sequences. Predicted transmembrane spanning domains for AgNHA1 are numbered and indicated by a red bar above the alignment. (B) A comparison of the hydropathy plots of the insect NHA1 amino acid sequences (TopPred II parameters were: GES-hydrophobicity scales; upper cut-off=1.0; lower cut-off=0.6; core window size=10; wedge window size=5; Critical loop length=60; and critical transmembrane spacer=2). Sequences were aligned relative to amino acid position (horizontal scale). Transmembrane-spanning regions predicted for AgNHA1 are indicated by the vertical red bars. Ae, *Aedes aegypti*; Ag, *An. gambiae*; Am, *Apis mellifera*; Ds, *D. pseudoobscura*; Dm, *D. melanogaster*; Tc, *Tribolium castaneum*.

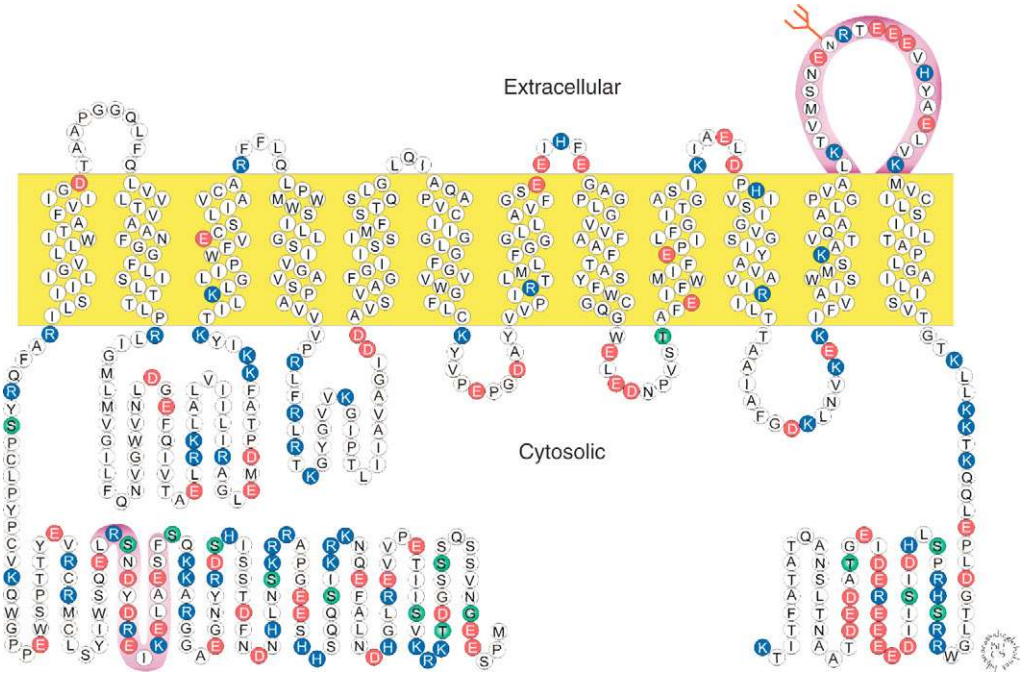

Fig. 2. Cartoon of the predicted secondary structure of AgNHA1. Color code for amino acids: positively charged, blue; negatively charged, red; non-polar or zwitterionic, white. Putative phosphorylation sites, green, N-glycosylation sites, orange; antigenic sequences used for antibody production, purple.

(TMDs) and a 70-residue cytosolic C terminus (Figs 1 and 2). The 12 TMDs are conserved in all other insect NHAs except that of *Apis mellifera*, which lacks TMDs 1 and 2 (Fig. 1B). *Drosophila melanogaster* and *D. pseudoobscura* have one and two additional N-terminal TMDs, respectively.

The amino acid sequence of AgNHA1 predicts the Pfam:Na^+/H^+ exchanger domain that is commonly found in CPA proteins from L183 to S575, which includes TMDs 2–12. 18 phosphorylation sites are predicted, 15 of which are cytosolic and are putative phosphorylation sites (Fig. 2). Seven of these sites (S22, S47, S62, T450, S601, S605 and S610) are highly conserved in all of the insect NHA1 transporters. Two possible N-glycosylation sites were predicted for AgNHA1; of these N543 is in the extracellular loop between the 11th and 12th TMDs and is a candidate site for N-glycosylation (Fig. 2).

Alignment of AgNHA1 amino acid sequences and phylogenetic relationships

AgNHA1 has the highest identity (75%) with the NHA1 protein of its *Culicid* relative, *Aedes aegypti* (Table 2). *Culicidae* NHA1 protein sequences are 55–58% identical with their *Drosophilidae* counterparts. The coleopteran *Tribolium castaneum* NHA1 is 44–51% identical with its Dipteran counterparts. NHA1 of *Apis mellifera*, a Hymenopteran, has the lowest predicted identity (35–42%) with the other insect NHAs. The AgNHA1 protein shares only 19–24% identity with predicted insect NHA2 or vertebrate NHA1 and NHA2 proteins.

Table 2. *Comparison of AgNHA1 sequence identity with NHA1 and NHA2 proteins*

	AgNHA1	AeNHA1	DsNHA1	DmNHA1	TcNHA1	AmNHA1
AeNHA1	75%					
DsNHA1	58%	56%				
DmNHA1	56%	55%	89%			
TcNHA1	51%	49%	46%	44%		
AmNHA1	38%	37%	36%	35%	42%	
HsNHA1	21%	22%	19%	19%	21%	21%
AgNHA2	24%	25%	22%	21%	26%	23%
AeNHA2	24%	25%	21%	21%	25%	25%
DmNHA2	23%	22%	20%	20%	24%	22%
AmNHA2	19%	20%	17%	17%	18%	16%
HsNHA2	26%	27%	22%	22%	26%	23%

Values are expressed as pairwise comparisons of percent identity from a protein sequence alignment done in ClustalW. Abbreviations are the same as those used in Table 1.

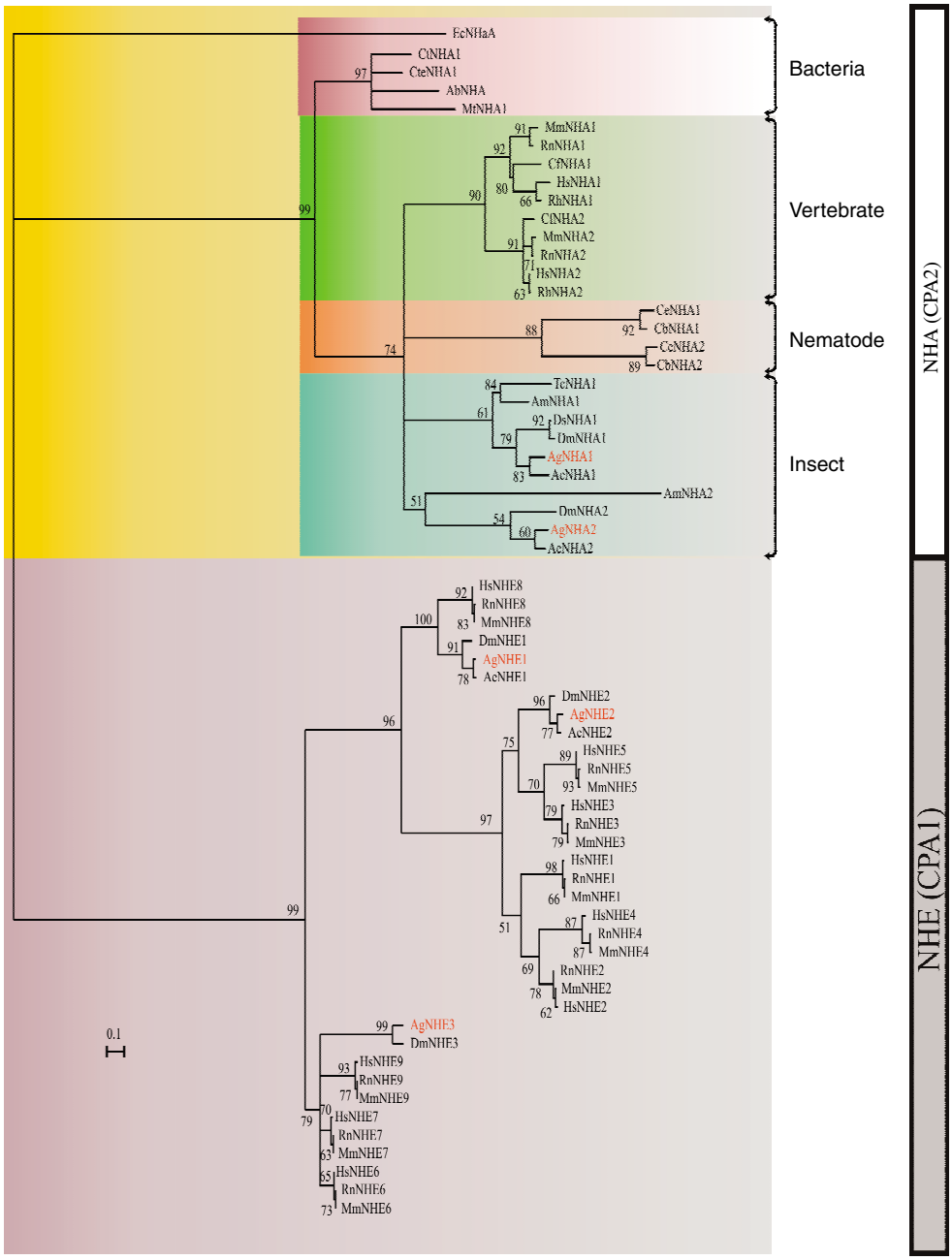

Fig. 3. Phylogenetic analysis of the cation proton antiporter (CPA) superfamily. The phylogenetic tree was constructed using maximum likelihood (ML) analysis and is shown as a ML-distance tree. It was deduced from an alignment of 65 sequences of prokaryotic and eukaryotic CPA genes and is arbitrarily rooted with the *E. coli* NhaA sequence. ML support values are shown at branch nodes. Background highlighting: CPA1 genes, purple; CPA2 genes, yellow; further CPA2 gene highlighting: bacteria, red; vertebrate, green; nematode, orange; insect, blue. The scale bar indicates the estimated number of amino acid substitutions per site. Abbreviations as in Table 1.

Moreover, the AgNHA1 protein shares only 3–8% identity with previously identified insect or vertebrate NHEs. In summary, AgNHA1 has high identity only with other insect NHA1s and far less identity with NHAs from other organisms; it has even less identity with all cloned NHEs, including those from *An. gambiae* and other insects.

In a phylogenetic analysis, AgNHA1 and other putative *Anopheles* CPA-like family members were compared (Fig. 3). 64 putative CPA transporter sequences were aligned, including 37 from vertebrates, 18 from insects, 4 from nematodes, and 5 from prokaryotes. The analysis revealed that *An. gambiae* genome contains five genes that appear to code for members of the CPA superfamily. These CPA members are separated into two distinct subfamilies (Fig. 3); AgNHE1 (XP_307859), AgNHE2 (AAO34131) and AgNHE3 (XP_314826) group with known members of the CPA1 (NHE) subfamily, whereas the newly cloned AgNHA1 (EF014219) and its relative AgNHA2 (XP_312647) group with the CPA2 (NHA) subfamily. Within the

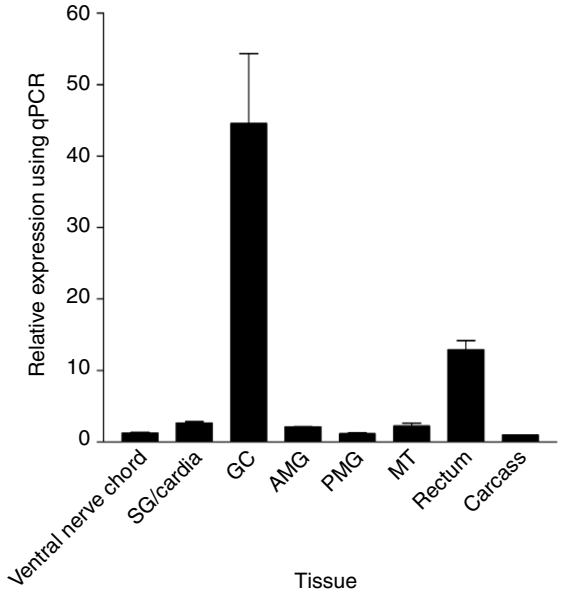

Fig. 4. qPCR analyses of AgNHA1 transcript expression in fourth instar larval tissues of *An. gambiae*. Data are presented as the mean + s.e.m. of three averaged replicates of three independent experiments. *An. gambiae* 18S ribosomal RNA was used as a reference gene. Results were normalized to values for carcass at one. VNC, ventral nerve cord; SG/cardia, salivary glands and cardia; GC, gastric caeca; AMG, anterior midgut; PMG, posterior midgut; MT, Malpighian tubules.

CPA1 subfamily the insect NHE1s are closely grouped with the NHE8s of vertebrates. Insect NHE2s are closest to the NHE3s and NHE5s of vertebrates and more distantly related to the NHE1s, NHE2s and NHE4s. Insect NHE3s are closest to vertebrate NHE6s, NHE7s and NHE9s. In contrast, within the CPA2 subfamily, AgNHA1 and AgNHA2 group together with other insect NHAs but not with vertebrate or non-insect counterparts. This isolation identifies AgNHA1 and AgNHA2 as possible targets for development of specific insect control agents.

Transcript abundance of AgNHA1 in larvae of An. gambiae

A relative profile of AgNHA1 expression in tissues from fourth instar larvae of *An. gambiae* was generated by qPCR using AgNHA1 gene-specific primers. The highest relative AgNHA1 expression was found in the gastric caeca and the rectum, although AgNHA1 mRNA was detectable at some level in all tissues tested (Fig. 4). *In situ* hybridization using full-length AgNHA1 DIG-labeled probes on whole mounts of fourth instar larvae confirmed that AgNHA1 is highly transcribed in both gastric caeca (Fig. 5B,C) and the rectum (Fig. 5B,D). In some *in situ* images it was localized to posterior midgut as well, where its relative abundance as measured by qPCR was similar to that in the carcass. The *in situ* hybridization protocol was not sensitive enough to visualize reliably the low transcript levels of AgNHA1 that were observed in other tissues using qPCR. These low transcript levels should not be interpreted to mean that AgNHA1 is not important in posterior midgut (PMG). As reported below, antibodies to AgNHA1 protein clearly labeled the apical membrane of PMG cells; apparently its targeting to this membrane is so specific that minimal levels of AgNHA1 mRNA in PMG translates into sufficient transporter protein for immuno-detection.

AgNHA1 transcript expression was also observed in the various ganglia of the ventral nerve cord (VNC), namely the caudal ganglion (Fig. 5E), the abdominal ganglia (Fig. 5F), and the subesophageal ganglion (Fig. 5G).

Western blot analysis of AgNHA1 antibody

SDS-PAGE of isolated *An. gambiae* membranes revealed distinct separation of many proteins of various molecular masses. When blots were probed by AgNHA1 antibodies, a single band was detected; it corresponds to a molecular mass of ~71 kDa, which agrees within experimental error with that

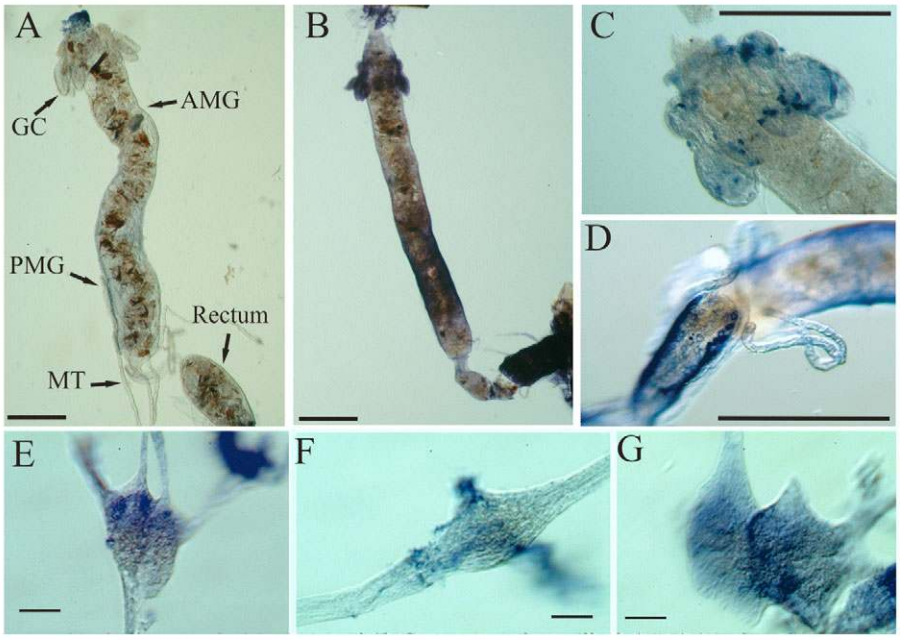

Fig. 5. The transcription patterns of AgNHA1 in tissues of fourth instar larval *An. gambiae*. AgNHA1 was detected by *in situ* hybridization using *in vitro* transcribed DIG-labeled antisense RNA of AgNHA1. Specific labeling appears purple or dark blue in color. The DIG-labeled sense control showed no specific staining (A). Expression of AgNHA1 transcript was observed in the gastric caeca, GC (B,C), posterior midgut (B,D) and the rectum (B,D). AgNHA1 transcript expression was also observed in the various ganglia of the ventral nerve cord (VNC). AgNHA1 was also expressed in the caudal ganglion (E), the abdominal ganglia (F) and the trilobed thoracic a.k.a. subesophageal ganglia (G). Scale bars, 500 μm (A–D); 75 μm (E–G).

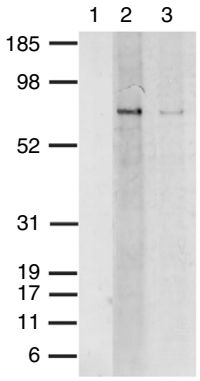

Fig. 6. Western blot of *An. gambiae* membrane proteins under reducing conditions. 25 μg of proteins were loaded in all lanes and subsequently probed with pre-immune serum in Lane 1, AgNHA1 antibody in Lane 2 and AgNHA1 antibody plus synthetic peptide (blocked antibody) in Lane 3. No protein was detected in the blot that was probed with pre-immune serum (Lane 1). Labeling of a single band in Lane 2 at the predicted molecular mass of 71 kDa shows that the antibody is specific for AgNHA1. Decreased signal in Lane 3 shows that the antibody is blocked by AgNHA1 synthetic peptide.

predicted for the AgNHA1 protein (Lane 2; Fig. 6). Probing the blots with pre-immune serum did not detect any bands (Lane 1; Fig. 6). Addition of a synthetic epitopic peptide blocked the AgNHA1 antibody-binding signal by nearly 20-fold, as quantified using ImageJ (Abramoff et al., 2004) (Lane 3, Fig. 6), confirming that the antibody is specific for AgNHA1.

Immunolocalization of AgNHA1 protein in larval An. gambiae

Immunolabeling of whole mounts of the larval mosquito alimentary canal revealed high expression of AgNHA1 in the cardia (Fig. 7A,B), gastric caeca (Fig. 7A–C), the anterior midgut (Fig. 7A,D), and proximal regions of the Malpighian tubules (Fig. 7A,E) as well as in portions of the rectum (Fig. 7A,F–H). In cardia, the antibody labeled a broad anterior band of small cells and a narrower band of larger cells closer to the GC, which do not appear to have been defined before. Lobes of cells in distal gastric caeca were intensely labeled (Fig. 7C), especially the Cap Cells (Smith et al., 2007). Within the body of the GC, a vesicular pattern of labeling was also observed (Fig. 7C). The labeling in the AMG was intense (Fig. 7A) and was mainly restricted to vesicles (Fig. 7D). Expression in PMG

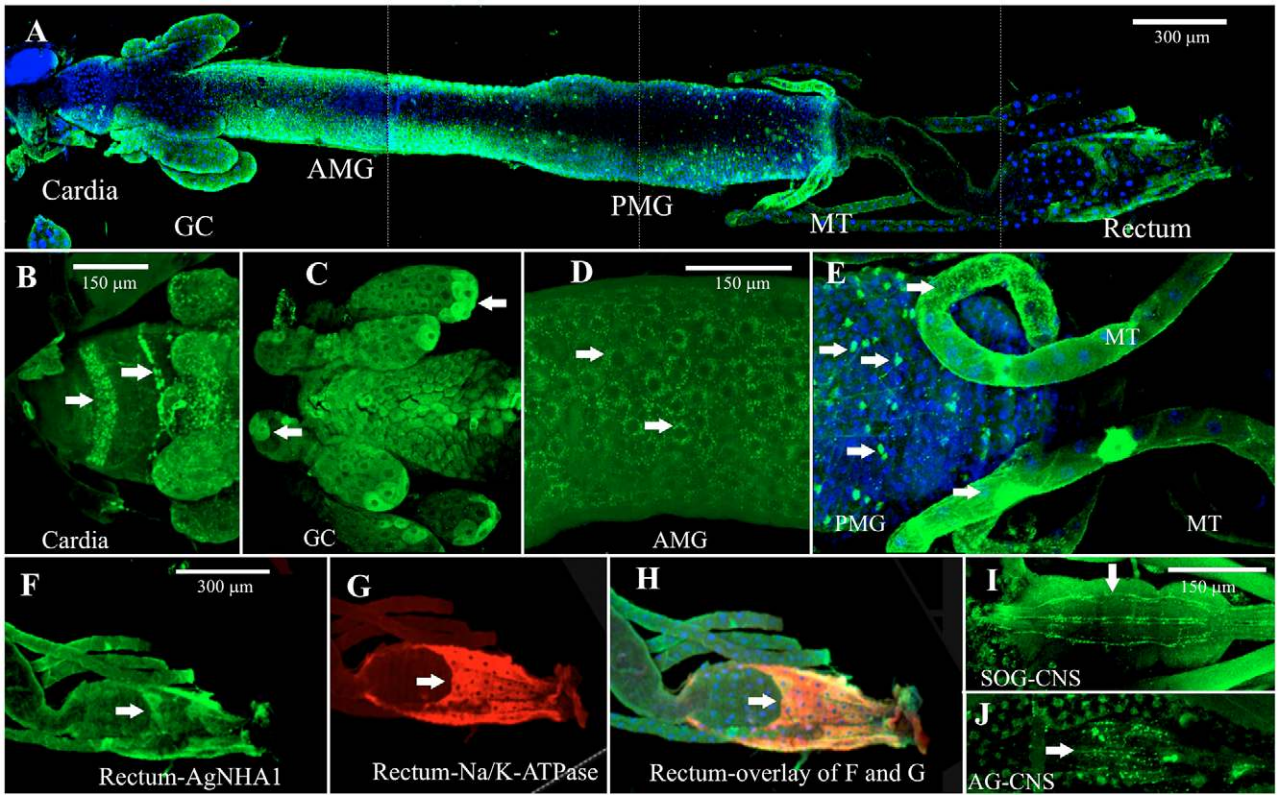

Fig. 7. Immunolocalization of AgNHA1 (green; FITC) and P-type Na^+/K^+ ATPase (red; TRITC) counterstained with a nuclear DNA marker (pseudo-blue; DRAQ-5) in isolated tissues of fourth instar *An. gambiae* larvae. (A) A composite whole mount, showing AgNHA1 expressed in the gastric caeca (GC), anterior midgut (AMG), selected cells of the posterior midgut (PMG), proximal Malpighian tubule (MT) and in a subset of cells in the rectum. (B) AgNHA1 was expressed in two bands of highly immunoreactive cells in the cardia. (C) AgNHA1 was highly expressed in the caudal tip of the gastric caeca. Scale in C is the same as B. (D) In the anterior midgut, AgNHA1 expression appeared to have a vesicular pattern of staining. (E) AgNHA1 stained cells (arrows) in the PMG and intensely stained cells in the proximal portion of the MTs (see arrow). Scale in E is the same as D. (F) AgNHA1 is expressed in the subset of cells in the rectum. AgNHA1 staining did not occur in the dorsal anterior rectal (DAR) cells. Similarly, Na^+/K^+-ATPase stained much of the rectum but did not stain its DAR cells (G). (H) An overlay of the AgNHA1 and Na^+/K^+-ATPase expression in the rectum. Colocalization of AgNHA1 and Na^+/K^+-ATPase in the same cells is indicated by the orange staining pattern. Scale in G,H is the same as F. In addition, AgNHA1 was expressed in the neuropil of the sub-esophageal ganglion (SOG) (I) and the abdominal ganglion (AG) (J). The scale in J is the same as in I.

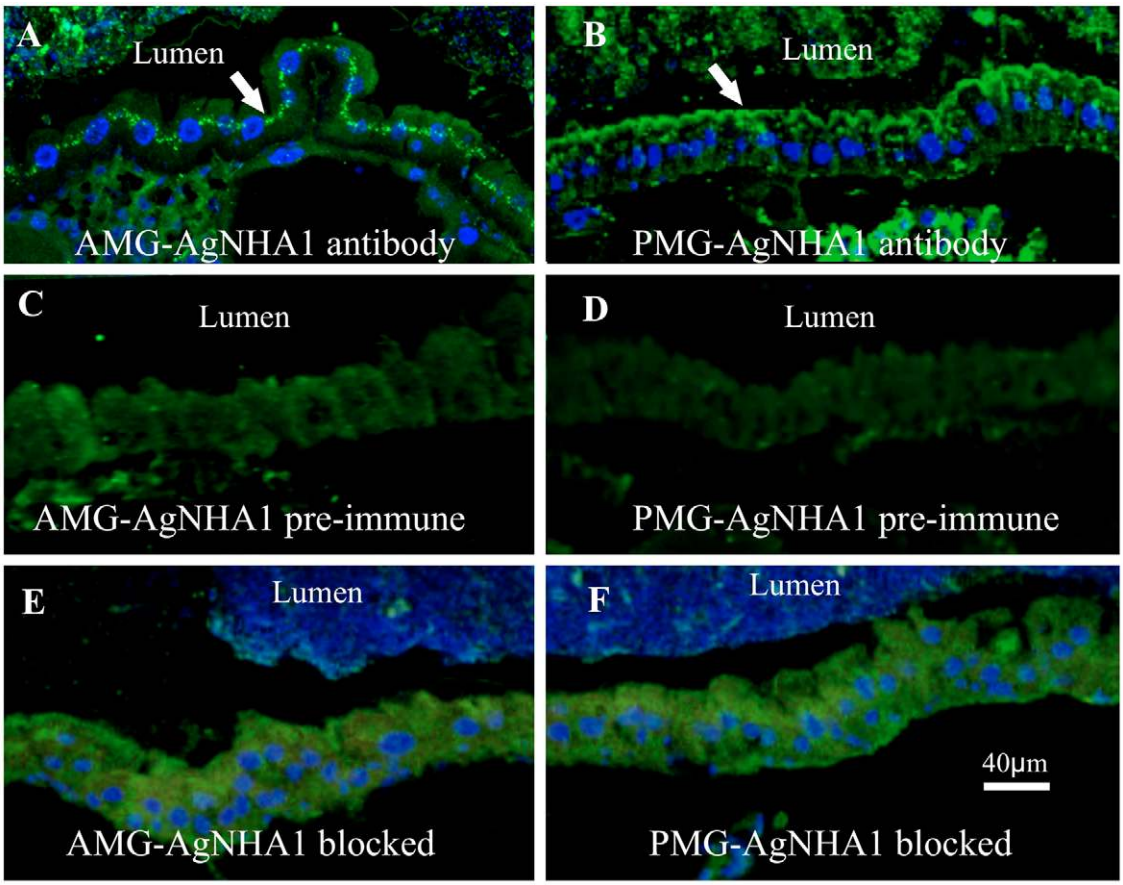

Fig. 8. Immunolocalization of AgNHA1 in mosquito midgut paraffin sections. (A) Vesicular staining pattern in the anterior midgut cells (AMG). In numerous sections the staining pattern appeared to be in line with the nucleus of the cell or just apical of the nuclei. (B) Apical localization of AgNHA1 in the posterior midgut cells. (C,D) Sections of AMG and PMG showing the lack of immunostaining by pre-immunization serum. (E,F) Sections in which the antibody was blocked by the AgNHA1 peptide; there was no specific staining other than background.

was limited to scattered cells that appear to be secretory in morphology (Fig. 7E, arrows). However, labeling was clear in paraffin sections of PMG, as discussed below (Fig. 8B,D,F). Labeling in the proximal fourth of the Malpighian tubules was intense and mainly in vesicles (Fig. 7E). The boundaries of posterior rectum were clearly defined by colocalization of AgNHA1 and Na^+/K^+ ATPase; however, the dorsal anterior rectal cells [DAR cells (Smith et al., 2007)] were not labeled by either antibody (Fig. 7F–H). High immunolabeling was also seen in the sub-esophageal and abdominal ganglia (Fig. 7I,J).

Immunolabeling of paraffin sections revealed details not seen in whole mounts but which may have profound physiological implications. First, in anterior midgut cells (Fig. 8A,C,E) a labeling pattern was observed that was restricted to a band of vesicles that lie between the nucleus and the apical plasma membrane (Fig. 8A). This vesicular pattern stretched from the anteriormost cells close to the gastric caeca to the transitional middle midgut region where the cell population shifts from a mostly cuboidal to a more columnar epithelial type. Second, in posterior midgut, AgNHA1 was clearly localized in the apical cell membranes that border on the ectoperitrophic space adjacent to the lumen (Fig. 8B,D,F). Although some intravesicular localization was also observed, it was restricted to cells that were close to the anterior midgut. The clear localization of AgNHA1 in apical membranes in posterior midgut cells contrasts to the limited AgNHA1 mRNA detected by qPCR (Fig. 4) and the failure to observe immunolabeling in whole mounts (Fig. 7E). This discrepancy underscores the value of cellular sections and the danger of relying solely on whole mounts in attempts to localize membrane transport proteins. No specific or distinct labeling patterns of AgNHA1 were observed in control experiments using the pre-immunization serum (Fig. 8C,D) or blocked antibody (Fig. 8E,F).

Discussion

AgNHA1 is the first cloned member of a new class of cation proton antiporters

Since Na^+/H^+ antiport was first identified in metazoans (Murer et al., 1976) and HsNHE1 was cloned and characterized (Sardet et al., 1989), many members of the NHE (CPA1) family have been studied in vertebrates (Orlowski and Grinstein, 1997; Orlowski and Grinstein, 2004) and a few in insects (see references below). By contrast, the NHA (CPA2) family has been virtually unexplored in metazoans, although NHAs have been identified in the genomes of vertebrates, insects and nematodes (Brett et al., 2005). Na^+/H^+ exchangers are all electroneutral, being driven by Na^+ gradients (cell concentration low) that translocate Na^+ into cells and H^+ out of them

Table 3. *Comparison of gene nomenclature used in Dipterans*

GenBank accession number	*Anopheles gambiae*[1]	Dipteran NHEs[2]	Amino acid sequence length	CPA gene family classification[1]
EF014219 (cloned)	NHA1	NHE10	647 (complete ORF)	CPA2/NHA
XP_312647 (predicted)	NHA2	NHE9	438* (predicted)	CPA2/NHA
XP_307859 (predicted)	NHE1	NHE8	549* (predicted)	CPA1/NHE IC NHE8-like
XP_319788 (predicted)	NHE2	NHE3	948* (predicted)	CPA1/NHE PM Recycling
XP_314826 (predicted)	NHE3	NHE6	674* (predicted)	CPA1/NHE IC Endo/TGN

[1](Brett et al., 2005).
[2](Pullikuth et al., 2003).
*Incomplete sequence.

(Grinstein and Wieczorek, 1994). The Na^+ gradients are set up by Na^+/K^+ P-ATPases, which from the mid-1970s were thought to energize all animal cell plasma membranes (Skou, 1990). However, since the mid-1980s, H^+ V-ATPases have been recognized as a second major class of animal plasma membrane energizers, which set up voltage gradients (cell negative) that drive secondary electrophoretic transporters (for reviews, see Wieczorek et al., 1999; Nelson and Harvey, 1999). In the post-genomic era the two ATPases and several electroneutral NHEs have been cloned and characterized from numerous organisms (Hart et al., 2002; Kang'ethe et al., 2007; Orlowski and Grinstein, 1997; Orlowski and Grinstein, 2004; Pullikuth et al., 2006) but the 'other shoe has never dropped' – no NHA has previously been cloned and localized in a metazoan organism, although they are present in every phylum for which a genome is available.

The phylogeny of CPA genes from dipterans

The five predicted *An. gambiae* CPA genes are distantly related to mammalian genes encoding Na^+/H^+ exchangers (NHEs; CPA1) and to both prokaryotic and eukaryotic (Na^+ or K^+)/H^+ antiporters (NHAs and KHAs; CPA2; Fig. 3). Brett et al. designated the five Dipteran CPA genes NHE1, NHE2, NHE3, NHA1 and NHA2 (Brett et al., 2005) and we have adopted these phylogenetically based names; see Table 3 for comparison of this nomenclature with that of Pullikuth et al. (Pullikuth et al., 2003).

Turning first to the NHE (CPA1) genes, AgNHE1 clusters with other Dipteran NHE1s, which are part of a larger cluster that includes vertebrate NHE8 homologs. NHE8 is widely expressed in vertebrate cells, where it is localized in plasma and endosomal membranes (Goyal et al., 2005; Orlowski and Grinstein, 2004). By contrast *Aedes aegypti* AeNHE1 (formerly AeNHE8), which is a homolog of vertebrate NHE8, is expressed solely in the apical membranes of the gastric caeca, Malpighian tubules and rectum (Kang'ethe et al., 2007). This discrepancy suggests that vertebrate NHE8s may function differently from insect NHE1s. Expression of AgNHE1 was not detected in the midgut epithelium of *Aedes*, however, and therefore it is not a likely candidate for the putative electrophoretic $K^+/2H^+$ antiporter that is discussed below (Kang'ethe et al., 2007).

AgNHE2 is most closely related to *Drosophila* NHE2 (Giannakou and Dow, 2001) and an *Aedes* NHE2 cloned by Hart et al. (Hart et al., 2002) [AeNHE3 (Pullikuth et al., 2006)]. The insect NHE3s cluster together with vertebrate homologs (NHEs 6, 7 and 9), suggesting that they are derived from a common ancestral invertebrate gene (Fig. 3). Vertebrate NHEs 1–5 are all electroneutral transporters, which exchange one extracellular Na^+ for one intracellular H^+ (Orlowski and Grinstein, 2004). NHE 7 is also electroneutral, but appears to exchange an extracellular K^+ for a H^+ *in vivo* (Numata and Orlowski, 2001). The physiological function and stoichiometry of the NHE6 and NHE8 homologs in vertebrates have yet to be elucidated.

The two remaining insect CPA genes, AgNHA1 and AgNHA2, belong to the CPA2 family (Brett et al., 2005), which are grouped as two separate clusters (Fig. 3). The insect NHA1 and NHA2 clusters share little identity to each other or to the vertebrate NHA clusters. This lack of identity between insect and vertebrate NHAs suggests that they may be potential targets for insect-specific control measures. By contrast, the close identity of insect NHEs with their vertebrate counterparts (Fig. 3) suggests that cross-specific toxicity may limit their value as control targets.

All of the animal NHAs appear to be more closely related to bacterial NHAs than to NHEs (Fig. 3). Bacterial NHAs have been shown to be energized by the voltage gradient provided by the H^+ F-ATPase and to transport two extracellular hydrogen ions for a single intracellular sodium or potassium ion, thus allowing them to survive in high saline and alkaline environments. It is natural to inquire whether insect NHAs in cell membranes adjacent to highly alkaline environments, such as the apical membranes in midguts of mosquito larvae or caterpillars, may have physiological functions that are analogous to those of NHAs in cell membranes of alkalophilic bacteria.

Freshwater animals, caterpillars and alkalophilic bacteria use H^+ V- or F-ATPases

Although all vertebrate NHEs are thought to be driven by Na^+ activity gradients, many vertebrates such as frogs live in freshwater with extremely low Na^+ concentrations (<1 mmol l^{-1}). Moreover, many herbivorous animals feed on plants containing little Na^+. It may be difficult for freshwater animals and herbivores to generate Na^+ gradients to drive their exchangers. Alkalophilic bacteria have the opposite problem: Na^+ leaks into the cells and is expelled against a Na^+ gradient by exchange with external H^+ *via* an NHA that is driven by the outside-positive voltage generated by an H^+ F-type ATPase (Padan et al., 2001). Caterpillars are faced with a problem similar to that of these bacteria except that K^+ rather than Na^+ is the offending alkali metal ion; massive amounts of K^+ are co-transported into the posterior midgut cells as nutrient amino acids are absorbed

(Giordana et al., 2002; Giordana et al., 1984; Giordana et al., 1998). Is it possible that freshwater-dwelling vertebrates and phytophagous insects, like alkalophilic bacteria, use a voltage gradient rather than a Na^+ gradient to drive their solute carriers? The answer is yes in the case of frogs and caterpillars. An H^+ V-ATPase in the much-studied frog skin mitochondria-rich cells generates a pond-side-positive voltage that is thought to drive sodium ions inwardly (Ehrenfeld and Klein, 1997; Larsen et al., 1987). Similarly, a H^+ V-ATPase in the caterpillar midgut generates a lumen-side-positive voltage that is thought to drive $2H^+$ into the cells and K^+ out to the lumen *via* a $K^+/2H^+$ antiporter (Wieczorek et al., 1991). An extensive unpublished study (B.A.O., D.Y.B. and W.R.H.) provides direct evidence that the localization of AgNHA1 is consistent with its energization by an H^+ V-ATPase. Indirect clues are provided here.

Clues regarding AgNHA1 function from transcription and protein expression patterns

AgNHA1 RNA is detected in tissues of gastric caeca, anterior midgut, posterior midgut and rectum. An antibody to AgNHA1 protein reveals cellular details. In cardia there are two bands of cells that express AgNHA1, neither of which has an identified function. In posterior gastric caeca, AgNHA1 expression appears to localize to a defined set of 'Cap Cells' (Smith et al., 2007), previously identified by Volkmann and Peters (Volkmann and Peters, 1989a; Volkmann and Peters, 1989b) as 'transporting cells'. It is possible that AgNHA1 may play a role in exchanging H^+ near the caecal plasma membrane for Na^+, thereby initiating the alkalinization process. AgNHA1 protein is also expressed in the anterior midgut of *Anopheles* larvae, where it appears as a broad band of vesicles between the nuclei and the apical plasma membrane (Fig. 7D and Fig. 8A). These locations are consistent with the notion that AgNHA1-containing vesicles could be incorporated into the apical membrane and participate in the alkalinization of the midgut under physiological stress, such as increased acidification of the midgut lumen. This sub-apical distribution is reminiscent of that in collecting ducts of mammalian renal tubules, where sub-apical vesicles containing V-ATPases fuse with the plasma membrane under 'acid stress' and extrude H^+ along with strong anions from metabolic acids (Brown, 1989; Brown and Sabolic, 1993; Brown and Stow, 1996).

Most exciting is the intense staining of the apical membrane of posterior midgut cells by the AgNHA1 antibody (Fig. 8B). This location is optimal for AgNHA1 to recycle the Na^+ that enters the cells along with nutrient amino acids *via* Na^+-coupled nutrient amino acid transporters (NATs) such as AgNAT8, which is located in this midgut region (Meleshkevitch et al., 2006). This massive influx of co-transported (symported) Na^+ would soon deplete the luminal Na^+ pool in the absence of an NHA. Fortuitously, an H^+ V-ATPase is colocalized in the same membrane with the NHA and NAT (B.A.O., D.Y.B. and W.R.H., unpublished data), where it could provide the voltage to drive both symporter and antiporter.

The heavy staining of proximal Malpighian tubules is consistent with their well-known role in reabsorbing solutes that have leaked into the lumen. Finally, AgNHA1 and Na^+/K^+ ATPase are dramatically colocalized in the rectum (Fig. 7F–H), where the larva recovers all remaining Na^+ from the lumen and avoids loss of scarce Na^+ to the dilute freshwater in which it lives (B.A.O., D.Y.B. and W.R.H., unpublished data). Finally, AgNHA1 is expressed in the ventral nerve cord of *Anopheles* larvae. Its function at this time remains to be elucidated, but we suggest that it may play a role in protecting the nervous system during periods of acid stress.

Is AgNHA1 the enigmatic $K^+/2H^+$ antiporter?

In the caterpillar midgut the lumen Na^+ concentrations are very low (Dow et al., 1984; Harvey et al., 1975), Na^+/K^+ P-ATPase cannot be detected and millimolar concentrations of ouabain fail to block cell functions (Jungreis and Vaughan, 1977). By contrast H^+ V-ATPase is highly expressed in the caterpillar midgut cells (Klein, 1992). More than two decades ago it was suggested (Dow, 1984) that the high pH in caterpillar midgut is achieved by '*stripping H^+ from luminal bicarbonate and moving it into the cells*'. Such a replacement of the weak H^+ cation by the strong K^+ cation in the caterpillar midgut lumen was proposed by Wieczorek and colleagues (Wieczorek et al., 1991), who provided convincing evidence that a $K^+/2H^+$ antiporter, operating in reverse, uses the positive luminal potential generated by a H^+ V-ATPase to move $2H^+$ from lumen to cell and $1K^+$ from cell to lumen (Azuma et al., 1995).

In larval *Aedes* mosquito midgut the driving force for (Na^+ or K^+)/H^+ exchange is electrical and the polarities of H^+ V-ATPase and Na^+/K^+ P-ATPase are the reverse of their usual locations (Zhuang et al., 1999). The force driving (Na^+ or K^+)/H^+ exchange also appears to be electrical in larval *An. gambiae* midgut, where an H^+ V-ATPase-generated voltage rather than a Na^+ chemical gradient appears to drive nH^+ into cells and Na^+ out of them (L. B. Popova, D.Y.B. and W.R.H., unpublished data). Remarkably, the situation is also similar between these insect larvae and certain alkalophilic bacteria. Thus, Lepier et al. noted that the main driving force for ion transport in the caterpillar midgut is the transmembrane voltage (Lepier et al., 1994). They observed that all prokaryotic Na^+/H^+ antiporters appear be electrophoretic (Taglicht et al., 1993). Prophetically they proposed that '*It is tempting to speculate that insect and bacterial cation/proton antiporters may be somewhat homologous*' and not a simple case of selective convergence. Indeed, the phylogram of the CPA subfamily (Fig. 3) shows that the insect NHAs are closer phylogenetically to bacterial NHAs than they are to vertebrate NHEs.

In summary, the midgut in both caterpillars and mosquito larvae shares three characteristics with alkalophilic bacteria: (i) the apical membrane is exposed to pH>10.5; (ii) this membrane is energized by electrogenic H^+-translocating F- or V-type ATPases, which are genetically related and functionally similar to each other; (iii) H^+ moves in and Na^+ moves out of the cells, the opposite of NHE-mediated ion movements in vertebrates. These data suggest that AgNHA1 is electrophoretically driven by an electrogenic H^+ V-ATPase and that it is the most likely candidate of all transporters thus far cloned to be the mosquito homolog of the long-sought-after caterpillar $K^+/2H^+$ antiporter.

Conclusions

More than half a century ago Ramsay (Ramsay, 1950) and others described an anterior–posterior pH gradient along the larval mosquito midgut that ranges from 7.5 in anteriormost

midgut to 8.3 in the gastric caecal cavity that opens into the midgut lumen. The pH approaches 11 in the anterior midgut, drops to 9.5 in middle midgut and falls rapidly to values from 6.2 to 7 in posterior midgut (Clements, 1992). The cloning and localization of AeNHE1 (Kang'ethe et al., 2007) and AeNHE2 (Pullikuth et al., 2006) from adult *Ae. aegypti* and that of AgNHA1 from larval *An. gambiae* reported here provide a core of structural data for finding how this gradient is generated and maintained.

Cloning AgNHA1 has much broader implications: just as NHEs catalyze electroneutral Na^+/H^+ exchange using the Na^+ chemical gradient generated by the Na^+/K^+ P-ATPase, we propose that NHAs catalyze electrophoretic Na^+/H^+ exchange using the voltage gradient generated by H^+ V-ATPases. This electrophoretic antiporter may play many roles in addition to pH and volume regulation. For example, it may play an essential role in Na^+ recycling during nutrient absorption in mosquitoes. The cloning of this first NHA can be expected to facilitate the study of CPA2 members throughout the animal phyla.

List of abbreviations

AC	alimentary canal
AG	abdominal ganglion
AgNHA	*Anophles gambiae* sodium ion/hydrogen ion antiporter
AgNHE	*Anopheles gambiae* sodium ion/hydrogen ion exchanger
AMG	anterior midgut
BLAST	Basic Local Alignment Search Tool
BSA	bovine serum albumin
CHA	cation/hydrogen ion antiporter
CHE	cation/ hydrogen ion exchanger
CPA1	cation proton antiporter 1
CPA2	cation proton antiporter 2
DAR	dorsal anterior rectum
DIG	digoxygenin
ELISA	enzyme linked immunosorbent assay
FITC	fluorescein isothiocyanate
GC	gastric ceaca
KHA	potassium ion/ hydrogen ion antiporter
KLH	keyhole limpet hemocyanin
ML	maximum likelihood
MR4	Malaria Research and Reference Reagents Resource Centre
MT	malpighian tubules
NaT-DC	sodium ion transporting carboxylic acid decarboxylase family
NBT/BCIP	nitroblue tetrazolium/5-bromo-4-chloro-3-indolyl-phosphate
NGS	normal goat serum
NHA	sodium ion/hydrogen ion antiporter
NHE	sodium ion/hydrogen ion exchanger
ORF	open reading frame
PBS	phosphate buffered saline
PBT	phosphate buffered saline with Triton X-100
PFA	paraformaldehyde in PBS
PMG	posterior midgut
qPCR	quantitative polymerase chain reaction
RACE	rapid amplification of cDNA ends
SG	salivary glands
SMART	Simple Modular Architecture Research Tool
SOG	sub-esophageal ganglion
TBS	Tris buffered saline
TBST	Tris buffered saline with tween 20
TMD	transmembrane domain
TRITC	tetramethyl rhodamine isothiocyanate
VNC	ventral nerve cord

This work was supported in part by an NIH Research Grant (AI 52436) to W.R.H., by a Natural Sciences and Engineering Research Council of Canada Postdoctoral Fellowship to M.R.R., and by the Whitney Laboratory for Marine Biosciences at the University of Florida.

References

Abramoff, M. D., Magelhaes, P. J. and Ram, S. J. (2004). Image processing with ImageJ. *Biophoton. Int.* **11**, 36-42.

Ahearn, G. A. and Clay, L. P. (1989). Kinetic analysis of electrogenic 2 Na^+ -1 H^+ antiport in crustacean hepatopancreas. *Am. J. Physiol.* **257**, R484-R493.

Ahearn, G. A. and Franco, P. (1991). Electrogenic $2Na^+/H^+$ antiport in echinoderm gastrointestinal epithelium. *J. Exp. Biol.* **158**, 495-507.

Azuma, M., Harvey, W. R. and Wieczorek, H. (1995). Stoichiometry of K^+/H^+ antiport helps to explain extracellular pH 11 in a model epithelium. *FEBS Lett.* **361**, 153-156.

Brett, C. L., Donowitz, M. and Rao, R. (2005). Evolutionary origins of eukaryotic sodium/proton exchangers. *Am. J. Physiol.* **288**, C223-C239.

Brown, D. (1989). Membrane recycling and epithelial cell function. *Am. J. Physiol.* **256**, F1-F12.

Brown, D. and Sabolic, I. (1993). Endosomal pathways for water channel and proton pump recycling in kidney epithelial cells. *J. Cell Sci. Suppl.* **17**, 49-59.

Brown, D. and Stow, J. L. (1996). Protein trafficking and polarity in kidney epithelium: from cell biology to physiology. *Physiol. Rev.* **76**, 245-297.

Chang, A. B., Lin, R., Studley, W. K., Tran, C. V. and Saier, M. H., Jr (2004). Phylogeny as a guide to structure and function of membrane transport proteins. *Mol. Membr. Biol.* **21**, 171-181.

Claros, M. G. and von Heijne, G. (1994). TopPred II: an improved software for membrane protein structure predictions. *Comput. Appl. Biosci.* **10**, 685-686.

Clements, A. N. (1992). *The Biology of Mosquitoes*. London: Chapman & Hall.

Dadd, R. H. (1975). Alkalinity within the midgut of mosquito larvae with alkaline-active digestive enzymes. *J. Insect Physiol.* **21**, 1847-1853.

Dow, J. A. T. (1984). Extremely high pH in biological systems: a model for carbonate transport. *Am. J. Physiol.* **246**, R633-R636.

Dow, J. A. T. and Peacock, J. M. (1989). Microelectrode evidence for the electrical isolation of goblet cell cavities in *Manduca sexta* middle midgut. *J. Exp. Biol.* **143**, 101-114.

Dow, J. A., Gupta, B. L., Hall, T. A. and Harvey, W. R. (1984). X-ray microanalysis of elements in frozen-hydrated sections of an electrogenic K+ transport system: the posterior midgut of tobacco hornworm (*Manduca sexta*) *in vivo* and *in vitro*. *J. Membr. Biol.* **77**, 223-241.

Ehrenfeld, J. and Klein, U. (1997). The key role of the H^+ V-ATPase in acid–base balance and Na^+ transport processes in frog skin. *J. Exp. Biol.* **200**, 247-256.

Gaillard, S. and Rodeau, J. L. (1987). Na^+/H^+ exchange in crayfish neurons: dependence on extracellular sodium and pH. *J. Comp. Physiol. B* **157**, 435-444.

Gasteiger, E., Hoogland, C., Gattiker, A., Duvaud, S., Wilkins, M. R., Appel, R. D. and Bairoch, A. (2005). Protein identification and analysis tools on the ExPASy server. In *The Proteomics Protocols Handbook* (ed. J. M. Walker), pp. 571-607. Totawa, NJ: Humana Press.

Gavel, Y. and von Heijne, G. (1990). Sequence differences between glycosylated and non-glycosylated Asn-X-Thr/Ser acceptor sites: implications for protein engineering. *Protein Eng.* **3**, 433-442.

Giannakou, M. E. and Dow, J. A. (2001). Characterization of the *Drosophila melanogaster* alkali-metal/proton exchanger (NHE) gene family. *J. Exp. Biol.* **204**, 3703-3716.

Giordana, B., Hanozet, G. M., Sacchi, V. F., Parenti, P. and Guerritore, A. (1984). Amino acid absorption in lepidopteran larvae midgut. *Boll. Soc. Ital. Biol. Sper.* **60 Suppl. 4**, 183-188.

Giordana, B., Leonardi, M. G., Casartelli, M., Consonni, P. and Parenti, P.

(1998). K(+)-neutral amino acid symport of *Bombyx mori* larval midgut: a system operative in extreme conditions. *Am. J. Physiol.* **274**, R1361-R1371.

Giordana, B., Forcella, M., Leonardi, M. G., Casartelli, M., Fiandra, L., Hanozet, G. M. and Parenti, P. (2002). A novel regulatory mechanism for amino acid absorption in lepidopteran larval midgut. *J. Insect Physiol.* **48**, 585-592.

Goyal, S., Mentone, S. and Aronson, P. S. (2005). Immunolocalization of NHE8 in rat kidney. *Am. J. Physiol.* **288**, F530-F538.

Grinstein, S. and Wieczorek, H. (1994). Cation antiports of animal plasma membranes. *J. Exp. Biol.* **196**, 307-318.

Grüber, G., Radermacher, M., Ruiz, T., Godovac-Zimmermann, J., Canas, B., Kleine-Kohlbrecher, D., Huss, M., Harvey, W. R. and Wieczorek, H. (2000). Three-dimensional structure and subunit topology of the V(1) ATPase from *Manduca sexta* midgut. *Biochemistry* **39**, 8609-8616.

Hart, S. J., Knezetic, J. A. and Petzel, D. H. (2002). Cloning and tissue distribution of two Na^+/H^+ exchangers from the Malpighian tubules of *Aedes aegypti*. *Arch. Insect Biochem. Physiol.* **51**, 121-135.

Harvey, W. R. (1992). Physiology of V-ATPases. *J. Exp. Biol.* **172**, 1-17.

Harvey, W. R., Wood, J. L., Quatrale, R. P. and Jungreis, A. M. (1975). Cation distributions across the larval and pupal midgut of the lepidopteran, *Hyalophora cecropia*, *in vivo*. *J. Exp. Biol.* **63**, 321-330.

Harvey, W. R., Cioffi, M., Dow, J. A. T. and Wolfersberger, M. G. (1983a). Potassium ion transport ATPase in insect epithelia. *J. Exp. Biol.* **106**, 91-117.

Harvey, W. R., Cioffi, M. and Wolfersberger, M. G. (1983b). Chemiosmotic potassium ion pump of insect epithelia. *Am. J. Physiol.* **244**, R163-R175.

Jungreis, A. M. and Vaughan, G. L. (1977). Insensitivity of Lepidopteran tissues to ouabain: absence of ouabain binding and Na^+–K^++ ATPases in larval and adult midgut. *J. Insect Physiol.* **23**, 503-509.

Kang'ethe, W., Aimanova, K. G., Pullikuth, A. K. and Gill, S. S. (2007). NHE8 mediates amiloride-sensitive Na^+/H^+ exchange across mosquito Malpighian tubules and catalyzes Na^+ and K^+ transport in reconstituted proteoliposomes. *Am. J. Physiol.* **292**, F1501-F1512.

Klein, U. (1992). The insect V-ATPase, a plasma membrane proton pump energizing secondary active transportimmunological evidence for the occurrence of a V-ATPase in insect ion-transporting epithelia. *J. Exp. Biol.* **172**, 345-354.

Larsen, E. H., Ussing, H. H. and Spring, K. R. (1987). Ion transport by mitochondria-rich cells in toad skin. *J. Membr. Biol.* **99**, 25-40.

Lepier, A., Azuma, M., Harvey, W. R. and Wieczorek, H. (1994). K^+/H^+ antiport in the tobacco hornworm midgut: the K^+-transporting component of the K^+ pump. *J. Exp. Biol.* **196**, 361-373.

Matz, M. V. (2002). Amplification of representative cDNA samples from microscopic amounts of invertebrate tissue to search for new genes. *Methods Mol. Biol.* **183**, 3-18.

Meleshkevitch, E. A., Assis-Nascimento, P., Popova, L. B., Miller, M. M., Kohn, A. B., Phung, E. N., Mandal, A., Harvey, W. R. and Boudko, D. Y. (2006). Molecular characterization of the first aromatic nutrient transporter from the sodium neurotransmitter symporter family. *J. Exp. Biol.* **209**, 3183-3198.

Murer, H., Hopfer, U. and Kinne, R. (1976). Sodium/proton antiport in brush-border-membrane vesicles isolated from rat small intestine and kidney. *Biochem. J.* **154**, 597-604.

Nelson, N. and Harvey, W. R. (1999). Vacuolar and plasma membrane proton-adenosinetriphosphatases. *Physiol. Rev.* **79**, 361-385.

Nicholas, K. B., Nicholas, H. B., Jr and Deerfield, D. W., II (1997). GeneDoc: analysis and visualization of genetic variation. *EMBNET News* **4**, 14.

Numata, M. and Orlowski, J. (2001). Molecular cloning and characterization of a novel $(Na^+,K^+)/H^+$ exchanger localized to the trans-golgi network. *J. Biol. Chem.* **276**, 17387-17394.

Orlowski, J. and Grinstein, S. (1997). Na^+/H^+ exchangers of mammalian cells. *J. Biol. Chem.* **272**, 22373-22376.

Orlowski, J. and Grinstein, S. (2004). Diversity of the mammalian sodium/proton exchanger SLC9 gene family. *Pflugers Arch.* **447**, 549-565.

Padan, E., Venturi, M., Gerchman, Y. and Dover, N. (2001). Na^+/H^+ antiporters. *Biochim. Biophys. Acta* **1505**, 144-157.

Padan, E., Bibi, E., Ito, M. and Krulwich, T. A. (2005). Alkaline pH homeostasis in bacteria: new insights. *Biochim. Biophys. Acta* **1717**, 67-88.

Page, R. D. M. (1996). TREEVIEW: an application to display phylogenetic trees on personal computers. *Comp. Appl. Biosci.* **12**, 357-358.

Patrick, M. L., Aimanova, K., Sanders, H. R. and Gill, S. S. (2006). P-type Na^+/K^+-ATPase and V-type H^+-ATPase expression patterns in the osmoregulatory organs of larval and adult mosquito *Aedes aegypti*. *J. Exp. Biol.* **209**, 4638-4651.

Pearson, R. B. and Kemp, B. E. (1991). Protein kinase phosphorylation site sequences and consensus specificity motifs: tabulations. *Meth. Enzymol.* **200**, 62-81.

Pullikuth, A. K., Filippov, V. and Gill, S. S. (2003). Phylogeny and cloning of ion transporters in mosquitoes. *J. Exp. Biol.* **206**, 3857-3868.

Pullikuth, A. K., Aimanova, K., Kang'ethe, W., Sanders, H. R. and Gill, S. S. (2006). Molecular characterization of sodium/proton exchanger 3 (NHE3) from the yellow fever vector, *Aedes aegypti*. *J. Exp. Biol.* **209**, 3529-3544.

Ramsay, J. A. (1950). Osmotic regulation in mosquito larvae. *J. Exp. Biol.* **27**, 145-157.

Sardet, C., Franchi, A. and Pouyssegur, J. (1989). Molecular cloning, primary structure, and expression of the human growth factor-activatable Na^+/H^+ antiporter. *Cell* **56**, 271-280.

Schlue, W. R. and Thomas, R. C. (1985). A dual mechanism for intracellular pH regulation by leech neurones. *J. Physiol.* **364**, 327-338.

Schmidt, H. A., Strimmer, K., Vingron, M. and von Haeseler, A. (2002). TREE-PUZZLE: maximum likelihood phylogenetic analysis using quartets and parallel computing. *Bioinformatics* **18**, 502-504.

Schultz, J., Milpetz, F., Bork, P. and Ponting, C. P. (1998). SMART, a simple modular architecture research tool: identification of signaling domains. *Proc. Natl. Acad. Sci. USA* **95**, 5857-5864.

Shetlar, R. E. and Towle, D. W. (1989). Electrogenic sodium–proton exchange in membrane vesicles from crab (*Carcinus maenas*) gill. *Am. J. Physiol.* **257**, R924-R931.

Sigrist, C. J. A., Cerutti, L., Hulo, N., Gattiker, A., Falquet, L., Pagni, M., Bairoch, A. and Bucher, P. (2002). PROSITE: a documented database using patterns and profiles as motif descriptors. *Brief. Bioinform.* **3**, 265-274.

Skou, J. C. (1990). The energy coupled exchange of Na^+ for K^+ across the cell membrane: the Na^+, K^+-Pump. *FEBS Lett.* **268**, 314-324.

Smith, K. E., Van Ekeris, L. A. and Linser, P. J. (2007). Cloning and characterization of AgCA9, a novel alpha-carbonic anhydrase from *Anopheles gambiae* Giles *sensu stricto* (Diptera: Culicidae) larvae. *J. Exp. Biol.* **210**, in press.

Strauss, O. and Graszynski, K. (1992). Isolation of plasma membrane vesicles from the gill epithelium of the crayfish, *Orconectes limosus* Rafinesque, and properties of the Na^+/H^+ exchanger. *Comp. Biochem. Physiol.* **102A**, 519-526.

Taglicht, D., Padan, E. and Schuldiner, S. (1993). Proton–sodium stoichiometry of NhaA, an electrogenic antiporter from *Escherichia coli*. *J. Biol. Chem.* **268**, 5382-5387.

Thompson, J. D., Gibson, T. J., Plewniak, F., Jeanmougin, F. and Higgins, D. G. (1997). The CLUSTAL_X windows interface: flexible strategies for multiple sequence alignment aided by quality analysis tools. *Nucleic Acids Res.* **25**, 4876-4882.

Umesh, A., Cohen, B. N., Ross, L. S. and Gill, S. S. (2003). Functional characterization of a glutamate/aspartate transporter from the mosquito *Aedes aegypti*. *J. Exp. Biol.* **206**, 2241-2255.

Volkmann, A. and Peters, W. (1989a). Investigations on the midgut caeca of mosquito larvae. I. Fine structure. *Tissue Cell* **21**, 243-251.

Volkmann, A. and Peters, W. (1989b). Investigations on the midgut caeca of mosquito larvae. II. Functional aspects. *Tissue Cell* **21**, 253.

von Heijne, G. (1992). Membrane protein structure prediction: hydrophobicity analysis and the positive-inside rule. *J. Mol. Biol.* **225**, 487-494.

Wieczorek, H. (1992). The insect V-ATPase, a plasma membrane proton pump energizing secondary active transport: molecular analysis of electrogenic potassium transport in the tobacco hornworm midgut. *J. Exp. Biol.* **172**, 335-343.

Wieczorek, H., Weerth, S., Schindlbeck, M. and Klein, U. (1989). A vacuolar-type proton pump in a vesicle fraction enriched with potassium transporting plasma membranes from tobacco hornworm midgut. *J. Biol. Chem.* **264**, 11143-11148.

Wieczorek, H., Putzenlechner, M., Zeiske, W. and Klein, U. (1991). A vacuolar-type proton pump energizes K^+/H^+ antiport in an animal plasma membrane. *J. Biol. Chem.* **266**, 15340-15347.

Wieczorek, H., Brown, D., Grinstein, S., Ehrenfeld, J. and Harvey, W. R. (1999). Animal plasma membrane energization by proton-motive V-ATPases. *BioEssays* **21**, 637-648.

Zhuang, Z., Linser, P. J. and Harvey, W. R. (1999). Antibody to H(+) V-ATPase subunit E colocalizes with portasomes in alkaline larval midgut of a freshwater mosquito (*Aedes aegypti*). *J. Exp. Biol.* **202**, 2449-2460.